Performance Prediction of the TMT Tertiary Mirror Support System

Myung K. Cho*

GSMT Program Office, National Optical Astronomy Observatory
950 N. Cherry Ave., Tucson, AZ 85719

ABSTRACT

The Ritchey-Chrétien (RC) optical design of Thirty Meter Telescope (TMT) calls for a 3.1m diameter secondary mirror (M2M) and an elliptical tertiary mirror (M3M) of 3.5m along its major axis and 2.5m along its minor axis. The M3M is a thin, large, flat, solid elliptical mirror which directs the f/15 beam from the M2M to the multiple instruments on both Nasmyth platforms. The M3M will weigh approximately two metric tons and the mirror support system will maintain the mirror figure at different gravity orientations. A recent reduction of the field of view to 15 arc minutes allows a reduction in the size of the M3M, which in turn requires re-optimization of the mirror support system. The proposed M3M optimized support system consists of 60 tri-axial supports mounted at the mirror back surface. These tri-axial supports accommodate motions of M3M in three gravity directions. The print-though RMS surface errors of M3M are 10nm for axial gravity loadings and 1nm for lateral gravity loadings. The M3 system (M3S) has an active optics (aO) capability to accommodate potential mechanical or thermal errors; its ability to correct low-order aberrations has been analyzed. A structure function (SF) of the axial gravity support print-through was calculated.

Keywords: Tertiary mirror, mirror performances, mirror support optimizations, active optics, Structure function

1. INTRODUCTION

The optical systems of TMT have stringent requirements, enabling the telescope to achieve its scientific goals. The M3M support system was optimized to meet the M3M shape requirements defined in "TMT Image Size and Wavefront Error Budgets" [3]. The wavefront error (WFE) budget allocation for M3M is 10nm RMS surface error over one beam footprint of elliptical area with major axis of 1.88 meters and minor axis of 1.33 meters. As a goal in the M3M support design and development, the requirement is defined over the entire M3M surface as 20nm RMS surface error with the telescope at Zenith, and 20nm RMS surface error with the telescope at 65 degrees elevation. To fulfill the optical and mechanical performance goals, extensive finite element (FE) analyses using I-DEAS and optical analyses with PCFRINGE have been conducted. Mechanical and optical analyses for static gravity induced deformations, natural frequency calculations, and support system sensitivity evaluations were performed. An influence matrix was established to compensate potential errors using an aO system. Performance of the M3 support system was evaluated for sample sensitivity cases before and after aO corrections.

The physical and material properties used in FE mirror models are summarized in Table 1.

Table 1. Material properties used in FE mirror models

Coefficient of thermal expansion	15×10^{-9} m/m°C
Thermal conductivity	1.3 W/m°C
Specific heat	766 J/kg°C
Density	2205 kg/m^3
Modulus of elasticity	9.2×10^{10} Pa
Poisson's ratio	0.17

* mcho@noao.edu; phone 1 520 318-8544; fax 1 520 318-8424; www.noao.edu

2. TERTIARY MIRROR CONFIGURATION

The M3M is a thin, large, flat, solid ellipse. The M3M directs the F/15 beam reflected from M2M to one of multiple instruments on either Nasmyth platform. A design concept of the M3 Cell Assembly (M3CA), developed by the National Optical Astronomy Observatory (NOAO), is shown in Figure 1(a). The thin solid mirror was adopted in order to smooth print-through bumps, corrected with adaptive optics (AO). Several different FE models were created for the different analyses. A typical FE mirror model consists of four layers of elements with a total of 10,080 solid elements and 12,245 nodes. This model assumes a thin solid flat mirror with a major axis of 2.506m, a minor axis of 3.522m, and a thickness of 100mm. The mass of the M3M is estimated at 1750Kg. The FE solid model is shown in Figure 1(b). The local coordinate system in the FE model is: (1) the positive Z-axis corresponds to the axis normal to the M3M surface; (2) the positive X-axis corresponds to the M3M mechanical tilt axis; (3) the positive Y-axis is defined by the right hand rule. This coordinate system used in the FE model is identical to that shown in Figure 2(a).

| (a) | (b) |
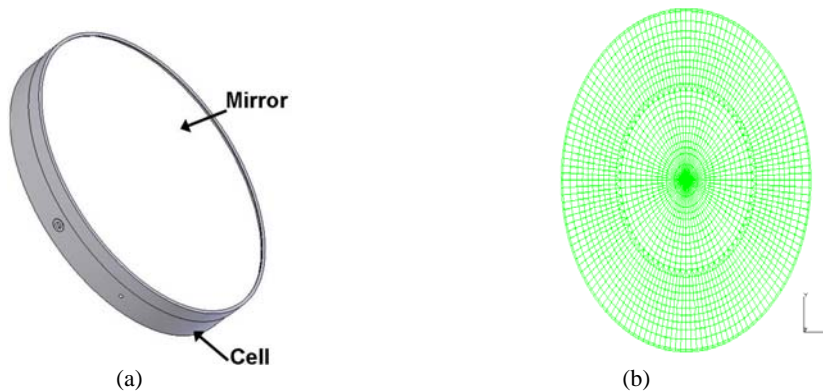
Fig. 1. (a) M3CA consisting of M3M, Support system, and Cell; and (b) M3M FE model (plane view of mirror).

3. M3M SUPPORT SYSTEM

As the telescope changes zenith angle, the M3S tracks in two axes to keep the beam aligned with an instrument. This implies that the M3M experiences gravity variations in all three orthogonal directions. The M3CA conceptual design was developed by NOAO to accommodate gravity variations resulting from the M3M motions as shown in Figure 2(a). The mirror support system contains a total of 60 tri-axial support actuators mounted at the back surface of the mirror. Shown in Figures 2(b) and (c) is a tri-axial design concept combining three individual supports inclined to one another such that their lines of action intersect at the mid-plane of the mirror. This tri-axial support arrangement is used passively for axial and both directions of lateral support.

Optimization of the support system design, for gravity affects on M3M, was performed at three orientations acting in the local X, Y, and Z-axes. The axial support system was optimized for the gravity in the local Z-axis, and the lateral was optimized at the gravity in the local X and Y, respectively. Each of these gravity orientations is outside the range of normal operations. The M3M support optimizations were made for a minimum global RMS optical surface error.

The aO system was established based on the influence matrix calculated from 60 axial support locations. To simulate low order aberrations, the natural mirror bending modes were modeled. The M3M aO system was applied to the mirror modes and the active optics performances were evaluated. It is essential to quantify the optical surface deformations affected by uncertainties in the design and potential errors involved in polishing, assembly and system integration. Support position errors, sample support failure modes, and random support force errors were simulated for the M3M support sensitivity and tolerance analyses. Detailed mechanical and optical performance analyses were conducted using the EDS I-DEAS finite element analysis program and the PCFRINGE optical program[7].

2
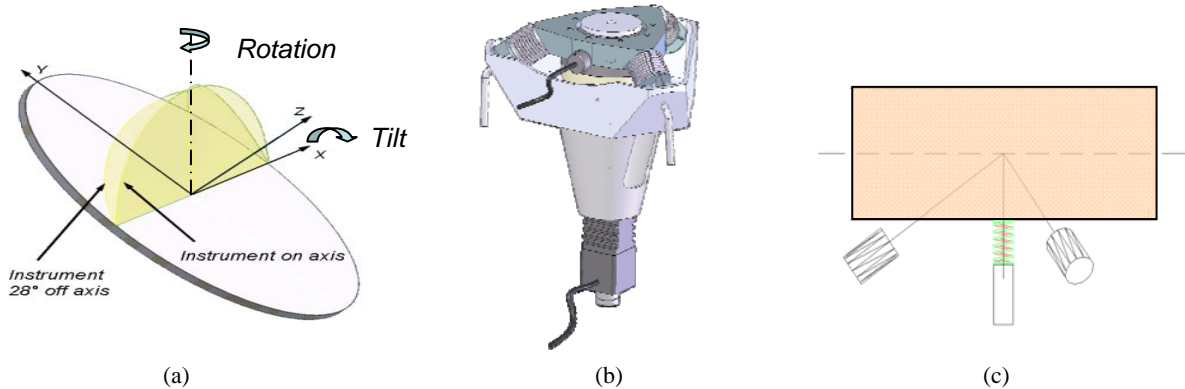
Fig. 2. (a) M3M motions (tilt and rotation) to align beam to the instruments, (b) design concept for a tri-axial support, and
(c) Illustration showing resultant support forces intersecting the mid-plane of M3M

3.1 M3M Axial Support

Parametric modeling iterations were conducted to optimize the design of the M3M support system. These iterative calculations utilize an optimization scheme for a minimum global RMS surface error over the optical surface. This optimization process was initially developed for the Gemini 8m telescopes [1] and applied to the Gemini primary mirrors.

Extensive parametric calculations were made in optimizing the axial support system to achieve the performance goal of 20nm RMS surface error. For the gravity in the local Z-axis, the axial support optimization yielded an RMS surface error of 11nm and 58nm P-V. This optimized support system features 60 axial supports arranged in a four (4) elliptical pattern (elongated hex-polar ring pattern). This support optimization involves two main optimization processes to achieve the goal. First, the support locations were determined for a minimum global RMS surface error without constraining support force magnitudes. Next, a further optimization was processed to select support forces into groups without sacrificing the RMS surface errors. Grouping supports will elevate manufacturing and design processes, and results in smaller part counts. The axial support forces were optimized in two groups, nominally 218~220N on the innermost ring and 276~306N on the rest. The optical surface contour map and the axial support forces (color coded for force magnitudes) are shown in Figures 3(a) and 3(b), respectively. Nine sub-apertures were constructed to simulate the print-through effects on M3M over the 15 arc minute field of view. Each of the nine sub-apertures was modeled over one beam footprint of elliptical area with major axis of 1.88 meters and minor axis of 1.33 meters. The surface map of each sub-aperture for the print-through and the RMS surface errors are shown in Figures 3(c) and 3(d). The M3M baseline axial support system descriptions and its configuration are summarized in Table 2.

Table 2. The axial support system configuration.

Ring	Radial position (ratio)	No. of Supports	Support Force Range (N)
1	17%	6	218~220
2	40%	12	276~306
3	63%	18	276~306
4	86%	24	276~306

3

(a)   (b)

(c)   (d)   (e)
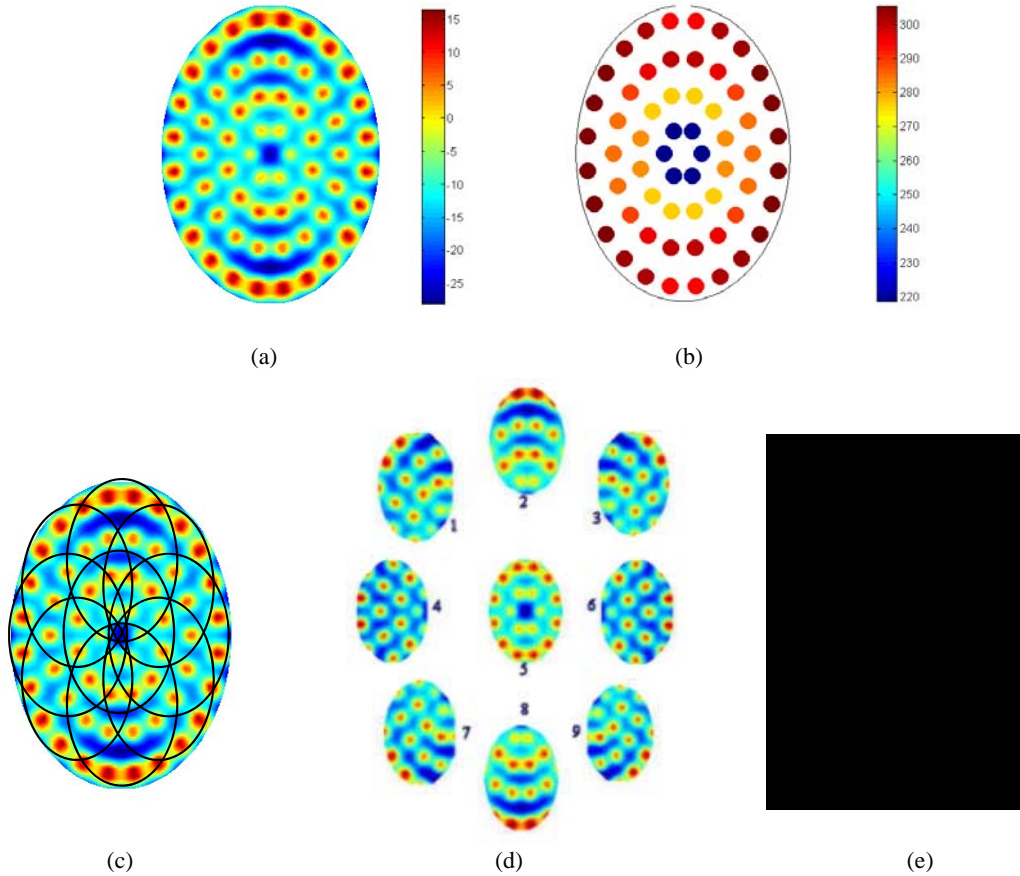
Fig. 3. (a) Axial support print through (RMS surface error =11nm over entire M3 surface), and (b) Axial support force in two groups (optimized support forces in different colors ranging from ~218N to ~306N), (c) Nine sub-aperture construction layout (d) Nine sub-aperture construction of axial support print-through, (e) RMS surface error for each of 9 sub-apertures. SA5 (center) is 9.0nm RMS surface error with M3M zenith pointing and becomes 6.4nm RMS surface error at telescope zenith pointing (M3M at 45 degrees), which is 9.0/sqrt(2).

3.2 M3M Lateral Support

The conceptual design of the passive TMT M3M lateral support system is to utilize the same 60 tri-axial supports used for the active axial support system. Since the lines of action in the tri-axial support intersect at the mid-plane of the mirror, the resultant support force due to the lateral gravity passes through the center of gravity (CG). This is equivalent to mounting the lateral supports at the CG location of M3M. If the system is perfect, then the global deformation from lateral support for a flat mirror would, theoretically, be zero. The optical surface errors due to the lateral gravity loading in the local X and Y-axes were calculated. The optical surface RMS errors are nominally 1 nm for both lateral cases. The optical surface error maps are shown in Figures 4(a) and 4(b), respectively.

TMT plans to have the support print through polished out for telescope zenith pointing; however, the negative of the axial support print through will gradually appear as the telescope moves away from the zenith. At a 65 degrees local Zenith position, the support gravity print-through would be a surface RMS of 7nm. Therefore, this M3M support system adequately meets the optical performance goal of 20nm RMS surface.

3.3 Support Sensitivity

Sensitivity and tolerance analyses were performed to quantify the optical surface deformations caused by uncertainties in the design and potential errors involved in polishing, assembly and system integration. Cases analyzed were: single support failure, single actuator force error, lateral support force errors, and random active force errors. For a sample axial

4

support failure mode, a single axial support on the fourth ring was assumed to fail, resulting in zero axial force. In this case, the net change of 44.2nm surface RMS error was calculated over the entire M3M surface after re-optimizing the remaining 59 active supports. The optical surface errors over the entire surface and 9 sub-apertures are shown in Figure 5. Similarly, for a case with a single axial support failure on the innermost ring, the net change of 12.8nm surface RMS error was calculated after re-optimizing the remaining 59 active supports. The optical surface errors over the entire surface and 9 sub-apertures are shown in Figure 6.
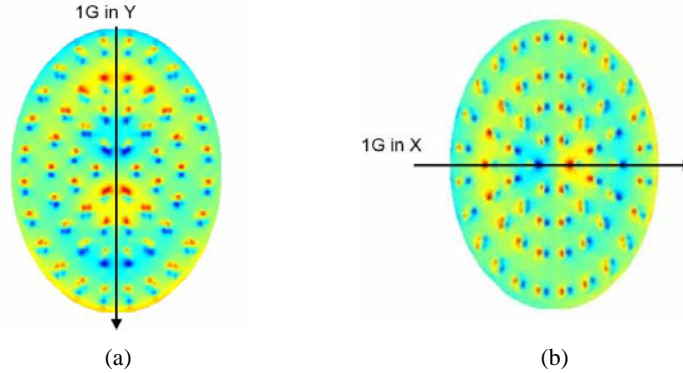
Fig. 4. (a) Lateral support print through due to gravity in the local Y-axis (RMS=1nm surface error), and (b) Lateral support print through due to gravity in the local X-axis (RMS=1nm surface error).
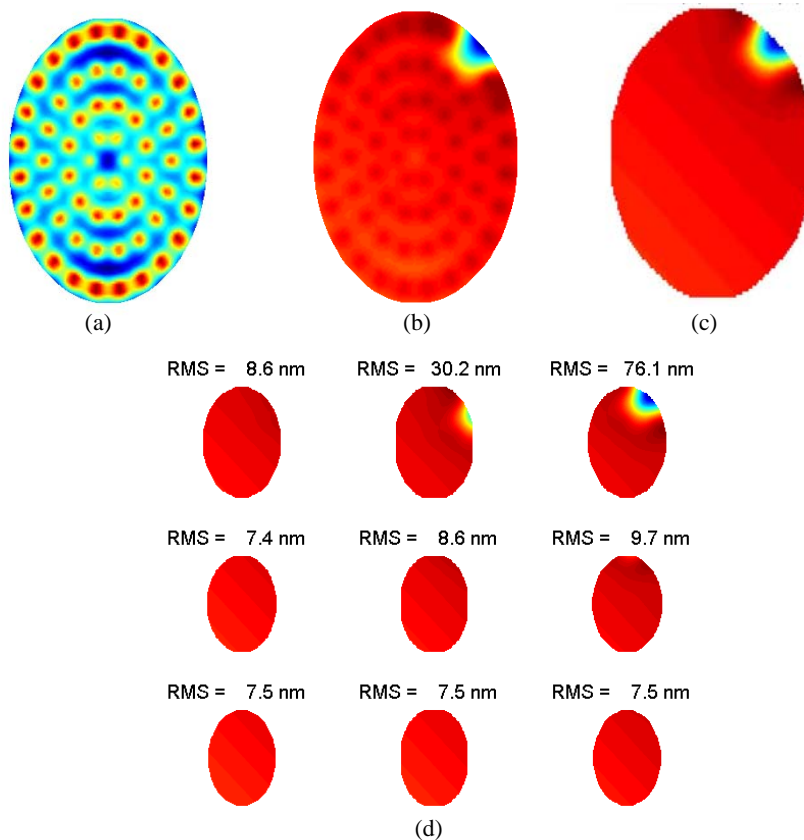
Fig. 5. The optical surface error due to a single support failure near the edge of M3M (aO system turned on). (a) Reference (undisturbed): Optical surface map, RMS = 10.9 nm. (b) Support failed: RMS = 44.5 nm. (c) Net changes: RMS = 44.2 nm surface error (entire surface). (d) Net changes: RMS surface error in 9 sub-apertures.

5

RMS = 20.4 nm   RMS = 22.5 nm   RMS = 22.6 nm

RMS = 12.6 nm   RMS = 22.0 nm   RMS = 22.0 nm

RMS = 7.4 nm   RMS = 6.9 nm   RMS = 16.3 nm

(a)   (b)
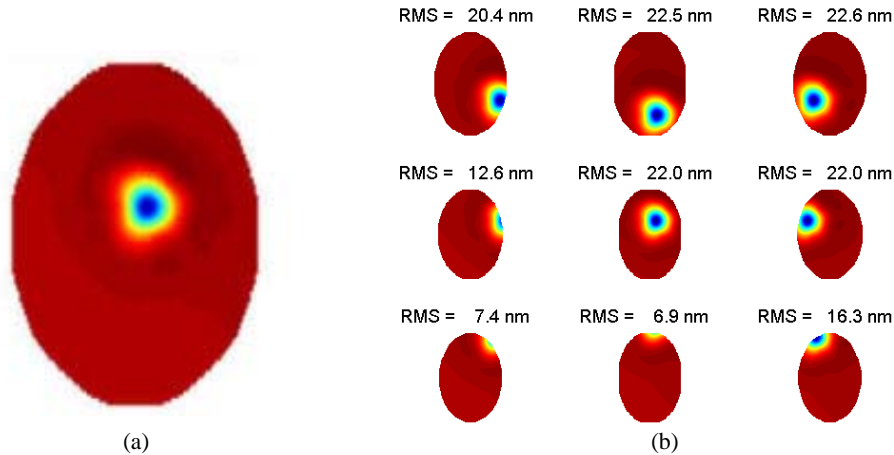
Fig. 6. The optical surface error due to a single support failure near center of M3M (aO system turned on).
(a) Net changes: Optical surface error map, RMS = 12.8 nm. (b) Net changes: Optical surface error maps of 9 sub-apertures.

For the case in which a single axial support has a force error of 1N, the net change in the optical surface RMS error is (after piston, tilts, and focus are removed) approximately 4nm, with an astigmatic shape. This can be used as a sample case to simulate a malfunctioning axial support actuator with a force error of 1N higher than required. Since we assume a linear FE analysis, the optical effect can be scaled linearly.

Further, the optical surface errors from support position errors are of interest. A case was considered, in which a single axial support actuator was misplaced (due to gravity in the local Z axis) by 1mm along the X and Y axes, as shown in Figure 7(a). A net change of a surface RMS error of approximately 0.1 nm was calculated. The optical surface error maps for both cases are shown in Figures 7(b) and 7(c).

(a)   (b)   (c)
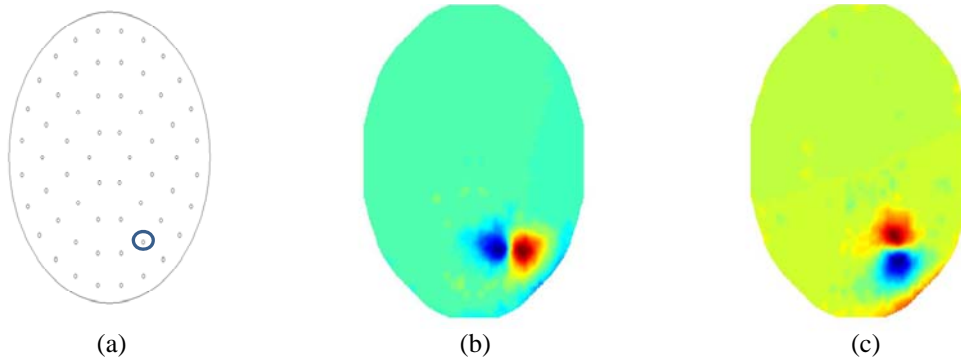
Fig. 7. Optical surface error map for 1mm of mis-position of an axial support actuator. Net change in optical surface RMS error for axial gravity loading is ~1nm. (a) single support mis-position shown in a circle, (b) Displaced 1 mm in X axis, and (c) Displaced 1mm in Y axis.

In addition, sensitivity effects were considered, of which the entire support system is misplaced or rotated about the Z axis (clocking) under the axial gravity load. This case can result from systematic errors during manufacturing and integration. Three cases were considered where the entire support was: (1) misplaced by 1mm along the X axis; (2) misplaced by 1mm along the Y axis; and (3) clocked by 1 milliradian. The net changes of the optical surface RMS error over the entire surface for these three cases are 0.7nm, 0.8nm, and 0.5nms, respectively. The optical surface error maps after removing piston, tilt, and focus are shown in Figures 8(a), 8(b), and 8(c), respectively.

The line of action of the lateral support force exerted by each lateral support lies on the mid-plane of the M3M. Any lateral support mis-position or excessive force will result in upsetting the force balance. For a case where a single lateral support actuator, on the third ring, is mis-positioned by 1mm along the optical axis (Z axis), an excessive moment of 0.286N-m (286N*0.001m) will be exerted on M3M. The net change in the optical surface RMS error, with gravity along

6

the local X-axis, is 2.6nm and 2.4 nm for the gravity along the local Y-axis. The optical surface errors, after piston, tilt, and focus removed, for the lateral gravity loadings are shown in Figures 9 (a) and 9(b).

(a)   (b)   (c)
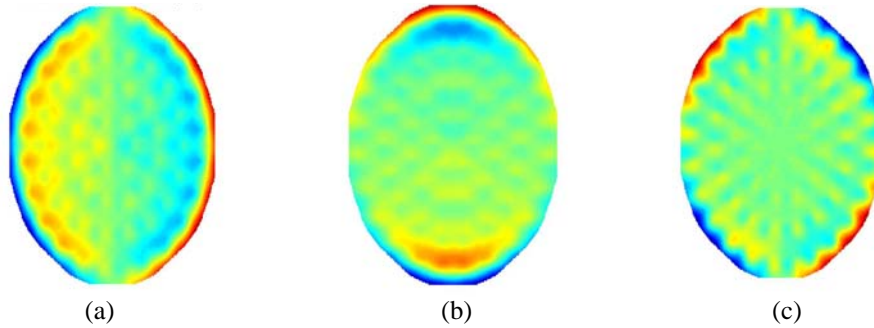
Fig. 8. Optical surface error maps. (a) RMS error = 0.7 nm due to entire axial support system mis-positioned by 1mm along the local X-axis. (b) RMS error = 0.8 nm due to entire support system mis-positioned by 1mm along the local Y-axis. (c) RMS = 0.5 nm due to entire support system clocked by 1 milliradian about the local Z-axis.

(a)   (b)   (c)
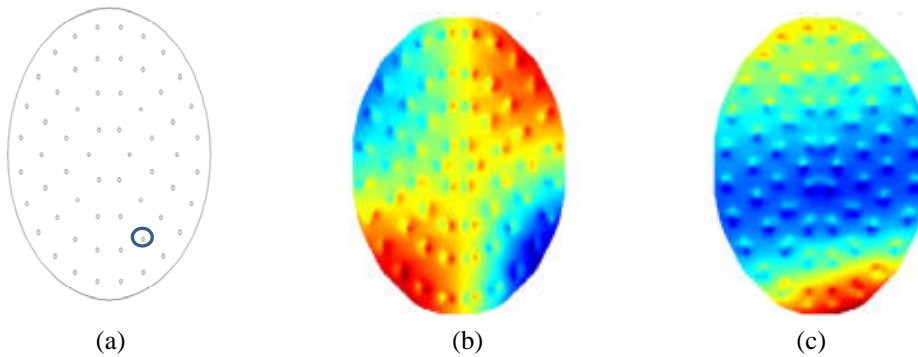
Fig. 9. Optical surface error maps where a single lateral support is mis-positioned by 1mm along the local Z-axis (piston). (a) single support mis-placed by 1mm shown in a circle (b) RMS error = 2.6 nm for gravity along the local X-axis. (c) RMS error = 2.4 nm for gravity along the local Y-axis.

Another interesting lateral support sensitivity case was modeled in which the entire lateral support was mis-positioned by 1mm along the local Z-axis. This results in an offset of 1mm between the line of action of the lateral support forces and the M3M mid-plane. In this case, an offset moment of 17.2N-m (60 of 286N*0.001m) will be exerted on M3M, due to lateral gravity loading. The net change in the optical surface RMS error = 36.5 nm for the gravity along the local X-axis and 34.5 nm for gravity along the local Y-axis. The optical surface errors, after piston, tilt, and focus are removed are shown in Figures 10(a) and 10(b). The resulting shapes are astigmatic, which can be corrected almost entirely by the M3M aO system.

(a)   (b)
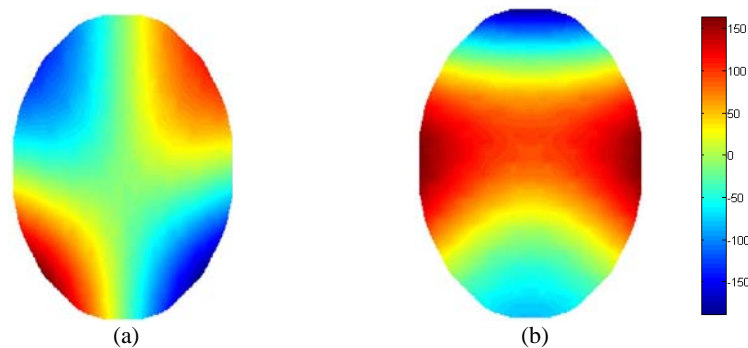
Fig. 10. Optical surface error maps. Errors are caused by one lateral support actuator mis-positioned by 1mm along the local Z-axis. (a) RMS error = 36.5 nm for gravity along the local X-axis. (b) RMS error = 34.5 nm for gravity along the local Y-axis.

7

Axial support force sensitivity calculations were made assuming that the axial forces are randomly distributed. This case can simulate actuator manufacturing errors, force repeatability, and limitations of force resolution. Ten different FE models were created with randomly distributed force errors on the actual support actuators. The distribution of the force errors was Gaussian with a random three-sigma value with a maximum axial force deviation of 0.5 N (+/- 0.25 N). A histogram of these 10 force distributions is shown in Figure 11(a) where each color represents a different distribution. The optical surface error maps produced by each force distribution (with piston, tilt, and focus removed) are shown in Figure 11(b). The optical surfaces errors for each model are listed in Figure 11(c). Results indicate an overall average of 3.4 nm RMS surface errors with predominantly astigmatic shapes.

| (a) | (b) | (c) |
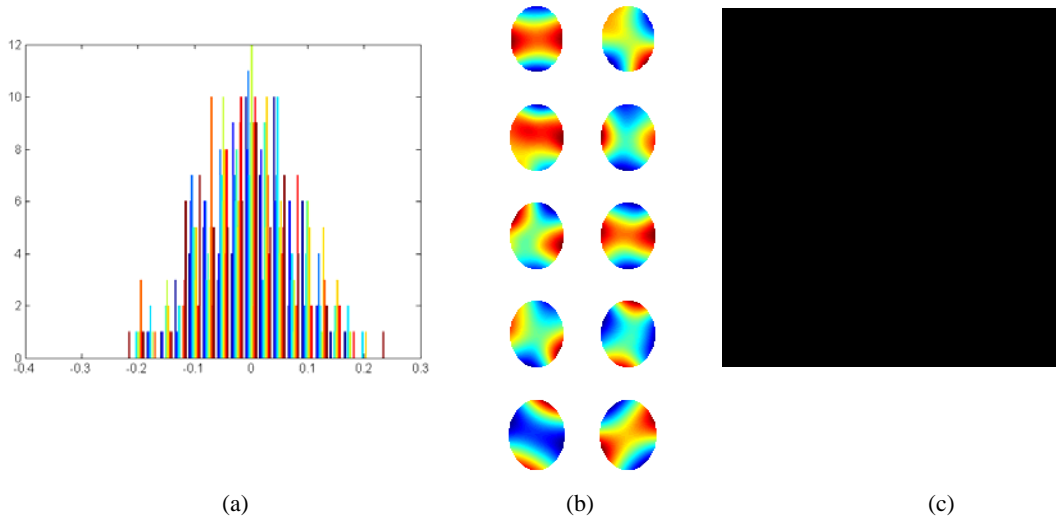
Fig. 11. Active optics force sensitivity (random axial actuator forces errors in Gaussian distribution). (a) Histogram of random forces for each of the 10 models where each color represents a different force profile distribution. (b) Optical surface error maps from the 10 FE modes. (c) Optical surface errors over entire mirror.

4. MIRROR FREQUENCY MODES

Natural frequencies of the mirror were calculated using a solid FE mirror model with a free-free boundary condition. These frequency modes are characteristic mirror bending shapes and were obtained after removing rigid body motions (piston and tilt). The natural frequencies, up to 24 modes, were calculated. The first 10 mode shapes are listed in Table 3, and shown in Figure 12. The lowest mode is at 60 Hz and is an astigmatic shape. The low frequency modes are similar to low order Zernike polynomials but not in the same order.

Table 3. First 10 Natural bending modes and frequencies.

mode ID	frequency (hz)	mode shape
1	60.3	0 astigmatism
2	70.9	45 astigmatism
3	132.9	focus
4	147.1	0 trefoil
5	155.9	30 trefoil
6	242.5	0 coma
7	262.5	0 quadfoil
8	267.9	45 quadfoil
9	328.5	90 coma
10	388.1	2nd coma

8
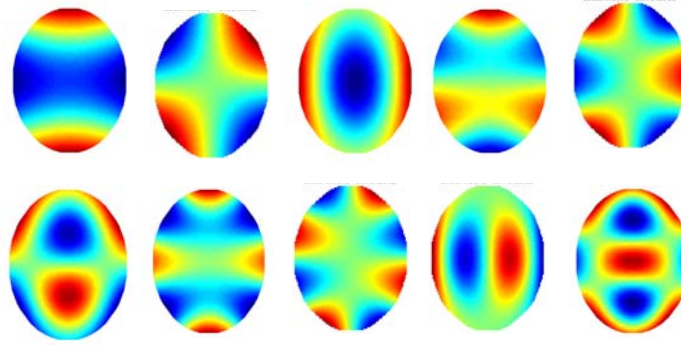
Fig. 12. Optical surface error maps from the first 10 Natural, free-free, bending modes listed in Table 3.

5. ACTIVE OPTICS PERFORMANCE

The M3M active optics (aO) system has 60 axial support actuators in the M3M support system. An influence matrix was constructed by calculating the influence function of each of the 60 axial support actuators. A 1 N force load was applied to one axial support actuator at a time. The M3M aO system will correct the M3M optical surface errors, open loop, using the influence matrix in a look-up-table (LUT). The M3M figure errors are mostly low order aberrations which can be decomposed into a set of low order orthogonal functions. Examples of orthogonal functions (sets) are Zernike polynomials, natural mirror bending modes, and modes from singular value decompositions (SVD).

The first 10 natural bending modes were modeled to evaluate the M3M aO performance. These are the same natural modes shown in Figure 12. Each of the first 10 modes was scaled to a RMS surface error of 1000nm as a reference. Active optics corrections were applied to each individual mode to minimum surface RMS error. Active optics correction capabilities for the mirror bending modes are summarized in Table 4. The maximum aO correction forces required to compensate each surface are listed along with the residual surface errors and the "gain", defined as the ratio of the RMS input amplitude (1000 nm in each case) to the residual RMS surface error. For example, the lowest mirror bending mode (Mode ID 1 in Table 4), is an astigmatic optical surface and can be corrected almost entirely. In this case, the astigmatism of 1000nm RMS surface error can be reduced to a residual RMS surface error of 0.3 nm with a maximum active force of 9.3 N. The gain, for this case, is 3897. The surface error map of this lowest mode and the aO force distribution are shown in Figure 13. Mode 10 is similar to a spherical aberration mode. The aO performance for this mode has only a gain of 43. The performance summary indicates that the M3M aO system works adequately with the low order aberration modes but does not perform as well for the higher order modes.

Table 4. Active optics performance with First 10 Natural bending modes.

	Input abberation		Active Optics Correction			
mode ID	P-V (nm)	rms (nm)	P-V (nm)	rms (nm)	Fmax (N)	Gain
1	3998	1000	2.4	0.3	9.33	3897
2	4583	1000	2.5	0.3	12.05	3457
3	4138	1000	7.3	1.1	40.48	880
4	5582	1000	18.0	1.8	56.04	557
5	4988	1000	14.2	1.6	60.90	608
6	4165	1000	37.4	6.2	113.01	162
7	5212	1000	56.4	6.3	173.47	159
8	5648	1000	52.0	5.7	190.30	174
9	4963	1000	55.8	7.5	226.02	133
10	4211	1000	139.8	23.4	438.25	43

9

(a)   (b)   (c)
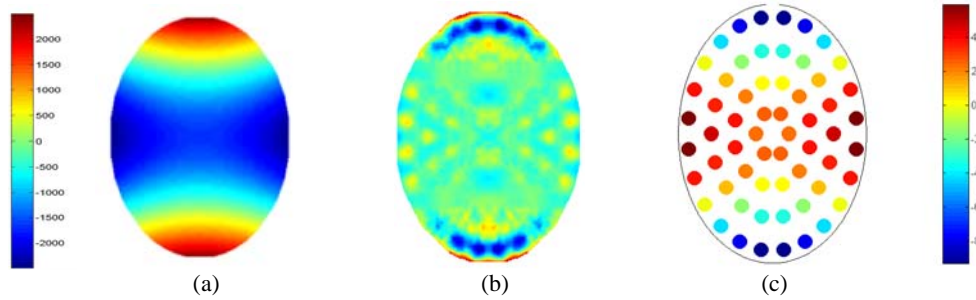
Fig. 13. aO correction for a surface RMS error of 1000nm of Astigmatism: RMS residual errors = 0.26 nm with maximum
aO force of 9.3 N. (a) Optical surface error map of Mode 1, RMS surface error = 1000 nm. (b) Residual RMS surface
error = 0.26 nm after aO correction. (c) aO system force distribution map (Fmax = 9.3 N).

The M3M aO support system is required to correct potential errors from external or internal loads after the M3CA is installed in the telescope. To demonstrate this capability, three cases were modeled to simulate the loading or environmental conditions that can exert forces on M3M. The three cases are as follows: (1) thermal gradients; (2) performance under Y gravity of mis-positioned lateral supports; and (3) performance under X gravity of mis-positioned lateral supports.

FE models were created with a 1-unit thermal gradient of $1^{o}C$ along each of the local coordinate directions on M3M to analyze thermal distortions due to temperature variations. A linear gradient of $1^{o}C$, along the thickness ($1^{o}C/0.1m$) with the top surface warmer by $1^{o}C$, was modeled. This is considered to be the most severe case. For this particular case, a P-V of 737 nm and RMS surface error of 182 nm were calculated, after removing piston and tilt. After applying aO correction, the optical surface RMS error was reduced to 4.3 nm, with a maximum aO correction force of 16 N. The surface error maps before and after the aO correction and the correction force distribution are shown in Figure 14. Note that insignificant RMS surface error (less than 1nm after removing piston and tilt) was calculated for thermal gradient cases along the local X or Y-axis before applying aO corrections.

(a)   (b)   (c)
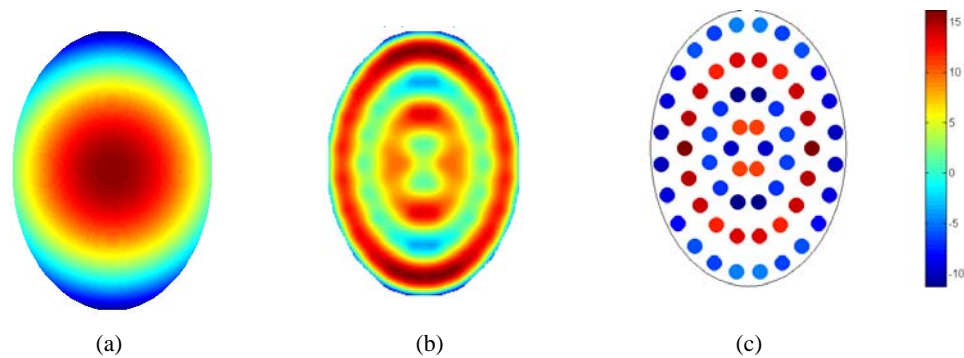
Fig. 14. aO correction for a thermal gradient through the thickness. (a) Optical surface error map from delta T = $1^{o}C$ over a
thickness of 0.1m , surface RMS error = 182 nm. (b) Residual RMS surface error = 4.3 nm. (c) Active optics force
distribution (Fmax = 16N)

As discussed in the lateral support sensitivity cases, the M3M was deformed noticeably into astigmatic shapes when the entire lateral support system was mis-positioned by 1mm along the optical axis, under lateral gravity loads. For the case where gravity is in the local X-axis direction, the M3M aO system can correct the 36.5 nm surface RMS error to 0.7nm, with a maximum correction force of 1.8 N. The surface error maps before and after the aO correction and the correction force distribution are shown in Figure 15. Similarly, for the case in where gravity is in the local Y-axis direction, the aO system can correct the 34.5 nm surface RMS error to 0.7nm, with a maximum correction force of 1.5 N. The surface maps before and after the aO correction and the aO force distribution are shown in Figure 16.

(a)   (b)   (c)
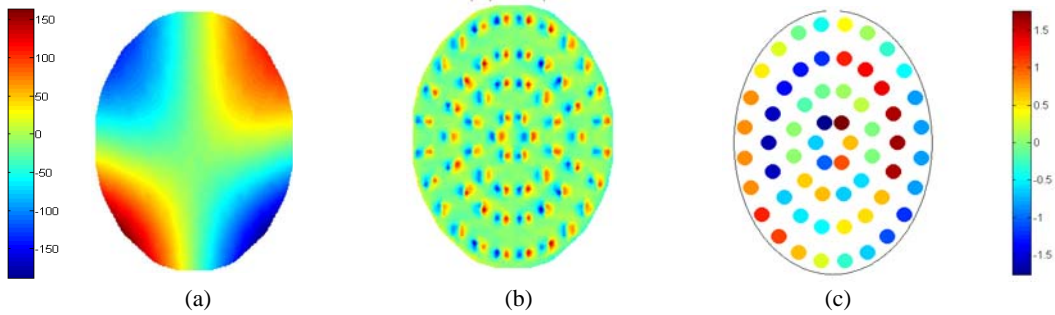
Fig. 15. aO correction for a lateral support position error by 1mm in Z, due to 1G in local X-axis direction. (a) Optical surface error map from gravity in local X-axis direction, surface RMS = 36.5 nm, (b) Residual RMS surface error = 0.7 nm, (c) Active optics force distribution (Fmax = 1.8N)

(a)   (b)   (c)
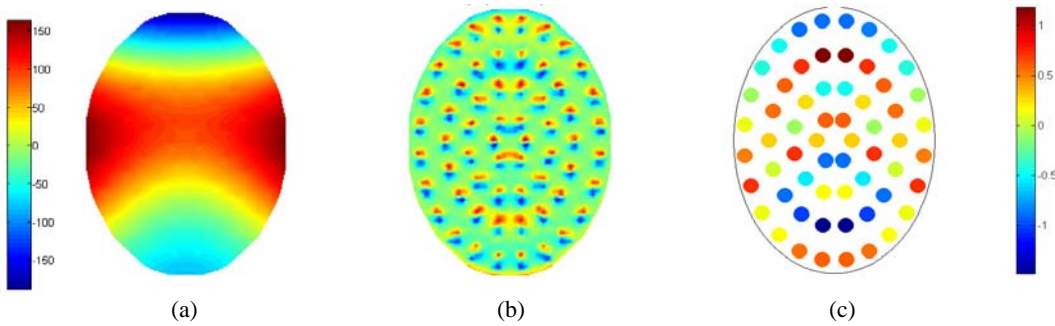
Fig.16. aO correction for a lateral support position error by 1mm in local Z-axis direction, due to 1G in local Y-axis direction. (a) Optical surface error map from gravity in local Y-axis direction, surface RMS error = 34.5 nm, (b) Residual RMS surface error = 0.7 nm, (c) Active optics force distribution (Fmax = 1.5 N).

6.   STRUCTURE FUNCTION

In order to control the amplitude of surface figure errors as a function of their spatial frequency, the M3S System Design Requirements Document (DRD) specifies the requirement for surface figure accuracy defined in terms of a Structure Function (SF). The value of SF for each separation distance is calculated in terms of the optical path difference (OPD) for each pair of points on the OPD map. SF is defined as: $D(r) = <[OPD(x + r) - OPD(x)]^2>$, where OPD is the OPD at a position x. A SF was calculated for the axial support print-through at all spatial scales and is shown in Figure 17. The OPD of the axial gravity was calculated when M3M is at a face up position, that is, the gravity is in the local Z-axis.
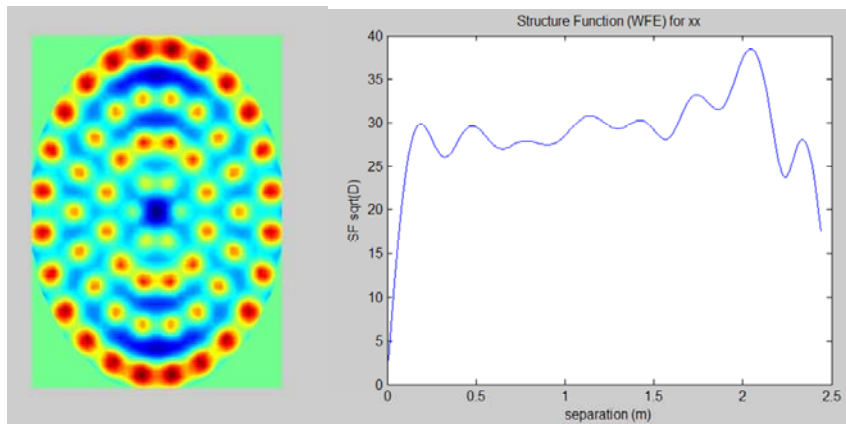
Fig. 17. OPD map of the axial gravity support print-through (22nm WFE) and the square root of the structure function, D(r), calculated from the OPD map, where: $D(r) = <[OPD(x + r) - OPD(x)]^2>$

11

In this case, OPD is twice the surface error. When the telescope is in Zenith and M3M is at 45 degrees, for example, the OPD will become cosine (45) of the axial gravity OPD with a scale factor of sqrt(2) for an incident beam angle of 45 degrees. The structure function of gravity print-through was compared to that of the atmospheric turbulence in the DRD. The gravity effect is favorably smaller than the atmospheric effect by approximately a factor of 10.

7. SUMMARY AND CONCLUSIONS

Extensive finite element analyses and opto-mechanical calculations were performed to optimize the TMT tertiary mirror support system. In the optimization process, iterative parametric analyses were utilized to achieve a minimum global RMS surface error. The axial support print-through for the optimized support system had an RMS surface error of 10nm. It used 60 tri-axial supports arranged in a four concentric ring (elongated hex-polar) pattern. The optimized lateral support system had an RMS surface error of nominal 1nm using the same 60 tri-axial supports with the resultant support force keeping on the mid-plane from lateral gravity loads. The optical surface errors for various Zenith angles were estimated by combining cases of the effects from the axial and lateral support actuators. The results indicated that the current TMT tertiary mirror support system adequately meets the optical performance requirements of 10nm RMS surface error over one beam footprint of elliptical area with major axis of 1.88 meters and minor axis of 1.33 meters. It also satisfies the M3M surface figure accuracy requirement defined in terms of a Structure Function.

Sensitivity analyses were conducted on several sample cases to quantify the optical surface errors caused by uncertainties in design and potential errors involved in manufacturing, polishing, assembly and system integrations. A summary of the sensitivity cases is listed in Table 5. All of these cases are before aO correction, except the first two cases. Note that the PV and RMS surface errors were calculated over the entire M3M optical surface. In addition, performance of the aO system was demonstrated by using the first 10 natural mirror bending modes. Table 6 shows several cases where the M3M aO system performance capability was demonstrated. The results demonstrated that the M3 active optics system is capable of adequately correcting the optical figure errors.

Integrated FE models with the mirror, supports, and mirror cell structure need to be established for further optimizations to refine design parameters of the mirror cell and support systems. A high fidelity finite element model will be required to evaluate more extensive sensitivity cases to evaluate the effects of structural interaction, thermal gradients, or other opto-mechanical effects. This FE model will include features of support pads, mounting blocks, linkage, and other detail hardware parts which can contribute to the degradation of mechanical and optical performance.

Table 5. Summary of sensitivity cases.

PV (nm)	RMS (nm)	REMARK
508.9	44.2	failure support at edge (after correction)
119.3	12.8	failure support at center (after correction)
16.0	4.0	single force center at edge (dF=1N)
1.1	0.1	single support mis-location (dx=1mm)
1.2	0.1	single support mis-location (dy=1mm)
5.0	0.7	support mis-placement (dx=1mm)
7.1	0.8	support mis-placement (dy=1mm)
4.1	0.5	support mis-placement (dr=1mrad)
14.5	2.6	single lateral force GX (dz=1mm)
14.2	2.4	single lateral force GY (dz=1mm)
195.8	36.5	lateral force position GX (dz=1mm)
163.0	34.5	lateral force position GY (dz=1mm)
16.1	3.4	random axial force error (dF=0.5N)

Performance Prediction of the TMT Tertiary Mirror Support System
TMT.OPT.JOU.08.002.REL01

Table 6. Active optics performance with First 10 Natural bending modes and sensitivity cases.

mode ID	Uncorrected P-V (nm)	Uncorrected rms (nm)	Active Optics Correction P-V (nm)	Active Optics Correction rms (nm)	Active Optics Correction Fmax (N)	Gain
0 astigmatism	3998	1000	2.4	0.3	9.33	3897
focus	4138	1000	7.3	1.1	40.48	880
0 trefoil	5582	1000	18.0	1.8	56.04	557
0 coma	4165	1000	37.4	6.2	113.01	162
0 quadfoil	5212	1000	56.4	6.3	173.47	159
90 coma	4963	1000	55.8	7.5	226.02	133
thermal gradient Z	737	182	21.0	4.0	16.20	46
lateral position GX	196	37	6.3	0.7	1.76	53
lateral position GY	163	35	5.6	0.7	1.43	49

REFERENCES

[1] Cho, M.K. and Price, R.S., "Optimization of Support Point Locations and Force Levels of the Primary Mirror Support System", RPT-O-G0017, Gemini Technical Report, November, (1993).

[2] Cho, M.K. and Roberts, J.L., "Response of the Primary Mirror to Support System Errors", RPT-O-G0021, Gemini Technical Report, November, (1993).

[3] Mast, T., "TMT Image Size and Wavefront Error Budgets Volume 1 2, 3", TMT.OPT.TEC.07.001, (2007).

[4] Blanco, D., Cho, M., Daggert, L., Daly, P., DeVries, J., Elias, J., Fitz-Patrick, B., Hileman, E., Hunten, M., Liang, M., Nickerson, M., Pearson, E., Rosin, D., Sirota, M. and Stepp, L., "Control and support of 4-meter class secondary and tertiary mirrors for the Thirty Meter Telescope," *Opt mechanical Technologies for Astronomy*, ed. E. Atad-Ettedgui, J. Antebi and D. Lemke, SPIE Proc. 6273, 2006; TMT.OPT.JOU.06.002, (2006).

[5] Cho, M.K, Performance Prediction of the TMT Tertiary Mirror, Ritchey-Chrétien design, TMT.OPT.TEC.07.026.REL01, (2007).

[6] TMT Optics Group, "TMT M3 System Design Requirement Document (DRD)", TMT.OPT.DRD.07.006.CCR28, (2007).

[7] Cho, M.K. and Richard, R.M., "PCFRINGE Program – Optical Performance Analysis using Structural Deflections and Optical Test Data", Version 3.5, the Optical Sciences Center, University of Arizona (1990).

13